J. Fluid Mech. (1972), *vol.* 54, *part* 4, *pp.* 641–663
Printed in Great Britain

The stability of a helical vortex filament

By SHEILA E. WIDNALL

Department of Aeronautics and Astronautics,
Massachusetts Institute of Technology

(Received 1 March 1972)

The stability of a helical vortex filament of finite core and infinite extent to small sinusoidal displacements of its centre-line is considered. The influence of the entire perturbed filament on the self-induced motion of each element is taken into account. The effect of the details of the vorticity distribution within the finite vortex core on the self-induced motion due to the bending of its axis is calculated using the results obtained previously by Widnall, Bliss & Zalay (1970). In this previous work, an application of the method of matched asymptotic expansions resulted in a general solution for the self-induced motion resulting from the bending of a slender vortex filament with an arbitrary distribution of vorticity and axial velocity within the core.

The results of the stability calculations presented in this paper show that the helical vortex filament has three modes of instability: a very short-wave instability which probably exists on all curved filaments, a long-wave mode which is also found to be unstable by the local-induction model and a mutual-inductance mode which appears as the pitch of the helix decreases and the neighbouring turns of the filament begin to interact strongly. Increasing the vortex core size is found to reduce the amplification rate of the long-wave instability, to increase the amplification rate of the mutual-inductance instability and to decrease the wavenumber of the short-wave instability.

1. Introduction

Recent advances in the understanding of the dynamics of curved vortex filaments makes it possible to re-examine the stability of basic vortex filament configurations such as the ring and the helix. In connexion with the study of the stability of the trailing vortex pair as a model for the aircraft wake, Widnall *et al.* (1970) presented a general solution for the self-induced motion of a curved vortex filament with an arbitrary (but stable) distribution of vorticity and axial velocity within the vortex core. (Hereafter this paper will be referred to as I.) This solution was then applied in the study of both the stability of the vortex pair and the self-induced motion of a vortex ring with an arbitrary vorticity distribution. The results obtained in the latter study agreed with the results obtained by Saffman (1970) from considerations of the energy and impulse of the ring. This solution for the self-induced motion of curved vortex filaments applies whenever the vortex core size is smaller than both the local radius of curvature and the wavelength of any perturbation along the filament.

The helical vortex filament is of intrinsic interest since it is one of the forms for which the self-induced motion of the filament will not distort the configuration; the helical vortex filament under its own influence will rigidly translate and rotate. In addition, helical vortex filaments are both found in, and used as, models for the wakes of helicopters and propellers. Convergence difficulties in the calculation of these wakes at small pitch angles indicate possible instability.

The small-perturbation analysis is, of course, only a first step in a more complete study which would include the induced motion due to large amplitude distortion of the helical filament. Owing to the complexity of this problem, direct attack using the digital computer to calculate the influence and motion of each point on the filament would be necessary. However, the proper numerical treatment of the finite vortex core and the examination of numerical as well as physical instability can now be based on the existence of an analytic solution.

A study of the stability of a helical vortex filament to small sinusoidal displacements of the centre-line of the vortex core was presented in 1928 by Levy & Forsdyke. In their treatment, a finite core was not explicitly considered and the singularity in the Biot–Savart law for the induced velocity on the filament itself was avoided by evaluating the integral at a point near the filament. The integrations were done using a planimeter. Unfortunately, the proper treatment of the finite vortex core is more subtle than the technique that they applied and consequently their results are in error, as will be seen later.

Betchov (1965) considered the stability of a helical vortex filament by applying the local-induction model, in which the self-induced velocity at a point on the filament is taken to be inversely proportional to the local radius of curvature in the direction of the local binormal to the curve and to be independent of effects from more distant elements of the vortex filament. The result of this analysis is that the helical filament is unstable for perturbation wavelengths longer than 2π times the local radius of curvature of the unperturbed filament and stable for shorter waves.

As will be seen, this mode of instability is also present when the full problem is considered but its amplification rate differs significantly from that predicted by the local-induction model. Beyond this, there are two additional modes of instability which are found when the effects of the entire filament are considered.

The theoretical investigation of the related problem of the stability of the vortex ring has been done and will appear when the companion experimental study has been completed (Widnall, S. E. & Sullivan, J. P. 1972 'On the stability of vortex rings', private communication). In this paper, this work is referred to as II. Some of the results of this study will be briefly discussed.

2. Formulation

The investigation of the stability of a helical vortex filament to small sinusoidal displacements of its centre-line proceeds by evaluating the self-induced velocities at the filament due to these perturbations. These induced velocities then kinematically determine the resulting motion of the filament and thus the growth rate

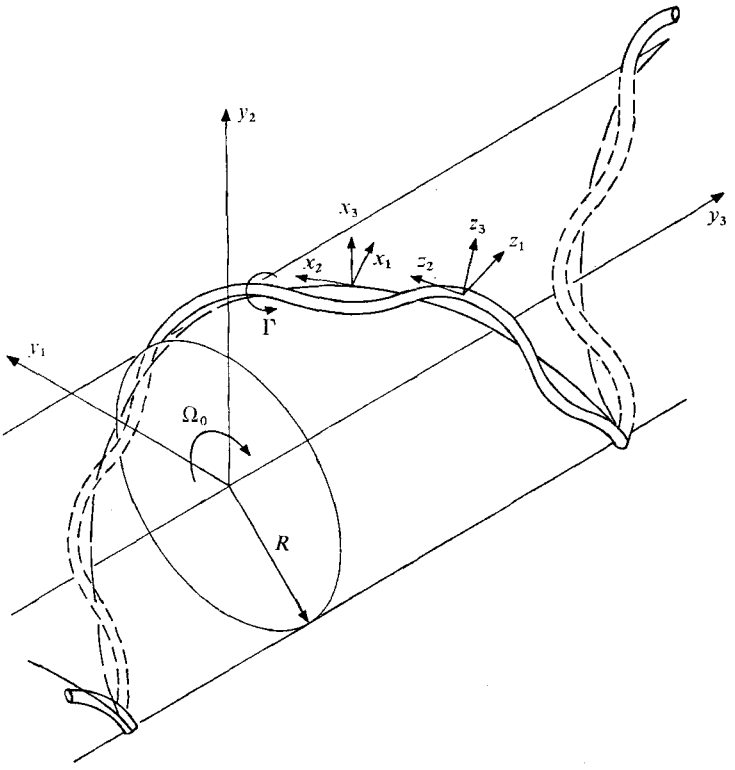

FIGURE 1. Sketch of the perturbed helical vortex filament showing the co-ordinate systems y_i, x_i and z_i.

(if any) of the perturbations. This analysis follows closely the similar analysis of the stability of the vortex ring (II), although the geometry for the helix is much more complex.

For a vortex filament of small core size the induced velocity at a point $\mathbf{y}'$ on the filament may be evaluated by a proper interpretation of the Biot–Savart law,

$$\mathbf{q}(\mathbf{y}') = \frac{\Gamma}{4\pi}\int_c \frac{(\mathbf{y}-\mathbf{y}')\times d\mathbf{y}}{|\mathbf{y}-\mathbf{y}'|^3}, \tag{1}$$

in terms of the vorticity distribution within the vortex core. This is done using results obtained in I, in which the local solution for a curved vortex filament of small core size was matched to the filament velocity from the Biot–Savart law (1) to give the self-induced motion of the filament.

The perturbed helical vortex filament is sketched in figure 1. The perturbations are taken as sinusoidal displacements normal to the filament in both the radial and tangential (i.e. along the cylinder) directions. (In the linearized stability analysis displacements along the filament are not considered.)

The stability problem is formulated in a co-ordinate system in which the unperturbed helix is stationary, i.e. a co-ordinate system which rotates with the angular velocity Ω_0 of the unperturbed helix and translates with the axial velocity V_A of the helix.

2.1. *Geometry of the perturbed filament*

Because of the potential geometric complications of the description of sinusoidal perturbations of a helical filament, we find it convenient and compact to work in curvilinear co-ordinates. We consider three co-ordinate systems: the first is the ordinary Cartesian system y_i, $i = 1, 2, 3$; the second is a curvilinear set x_i chosen so that the unperturbed helix is a co-ordinate curve $x_1 = 0$, $x_3 = R$ (the radius of the cylinder); the third is a curvilinear set z_i chosen so that the perturbed helix is a co-ordinate curve $z_1 = 0$, $z_3 = R$ (see figure 1).

The curvilinear co-ordinates $x_i = x_i(y_i)$ are defined by

$$\left.\begin{aligned} x_1 &= y_3 - (1/k)\tan^{-1}(y_2/y_1), \\ x_2 &= y_3 + R^2 k \tan^{-1}(y_2/y_1), \\ x_3 &= (y_1^2 + y_2^2)^{\frac{1}{2}}. \end{aligned}\right\} \tag{2}$$

This can be inverted to give $y_i = y_i(x_i)$. The unperturbed helix is given by the curve $x_1 = 0$, $x = R$. Although (2) defines a set of non-orthogonal co-ordinates, at $x_3 = R$ they are locally orthogonal. The pitch of the helix ($\tan\alpha$) is $1/Rk$.

The perturbations to the position of the filament are taken to be normal to the filament in the x_1 and x_3 directions. The perturbed filament is described by

$$x_1 = \xi_0 e^{i\gamma x_2}, \quad x_3 = R + \rho_0 e^{i\gamma x_2}, \quad x_2 = x_2, \tag{3}$$

where ξ_0 and ρ_0 are the amplitudes of the perturbations and γ is the wavenumber along x_2. (γ is not restricted to integer multiples of the wavenumber of the helix.)

The z_i co-ordinates are defined by

$$z_1 = x_1 - \xi_0 e^{i\gamma x_2}, \quad z_2 = x_2, \quad z_3 = x_2 - \rho_0 e^{i\gamma x_2}, \tag{4}$$

so that on the perturbed vortex filament $z_1 = 0$ and $z_3 = R$. The relation $y_i = y_i(z_j)$ can be found by eliminating x_i from (2) and (4) and solving for $y_i = y_i(z_j)$. For small values of ξ_0 and ρ_0 the Cartesian co-ordinates for a point on the perturbed filament are

$$\left.\begin{aligned} y_1 &= (R + \rho_0 e^{i\gamma z_2})\cos k'(z_2 - \xi_0 e^{i\gamma z_2}), \\ y_2 &= (R + \rho_0 e^{i\gamma z_2})\sin k'(z_2 - \rho_0 e^{i\gamma z_2}), \\ y_3 &= (z_2 + R^2 k^2 \xi_0 e^{i\gamma z_2})\zeta^2, \end{aligned}\right\} \tag{5}$$

where $\zeta = 1/(1 + k^2R^2)^{\frac{1}{2}}$ and $k' = k\zeta^2 = k/(1 + k^2R^2)$. The subscript on z_2 will be dropped from now on.

Equation (5) can be expanded in a Taylor series in ξ_0 and ρ_0 and written in column-vector notation as

$$\mathbf{y} = \begin{Bmatrix} R\cos k'z \\ R\sin k'z \\ z\zeta^2 \end{Bmatrix} + \xi_0 e^{i\gamma z} \begin{Bmatrix} Rk'\sin k'z \\ -Rk'\cos k'z \\ R^2k^2\zeta^2 \end{Bmatrix} + \rho_0 e^{i\gamma z} \begin{Bmatrix} \cos k'z \\ \sin k'z \\ 0 \end{Bmatrix}, \tag{6}$$

where the elements of the column vectors are the Cartesian components corresponding to $i = 1$, 2 and 3 respectively. The distance between any two points on the filament, say z and z', is just

$$\mathbf{y} - \mathbf{y}' = \mathbf{y}(z) - \mathbf{y}(z').$$

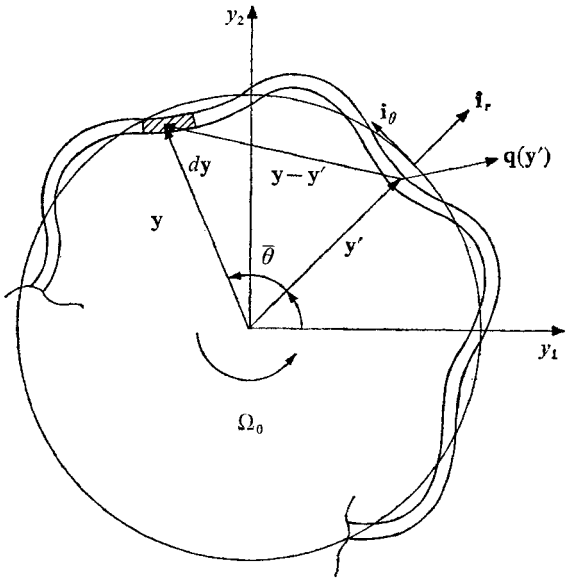

FIGURE 2. Cross-section of the perturbed helix showing the local unit vectors $\mathbf{i}_\theta$ and $\mathbf{i}_r$ and $\mathbf{y}'$.

The differential element $d\mathbf{y}$ of the filament is given by

$$d\mathbf{y} = (d\mathbf{y}/dz)\,dz = \mathbf{u}\,dz,$$

with $\mathbf{u}$ defined as $d\mathbf{y}/dz$. $\mathbf{u}$ in Cartesian components is obtained by differentiating (6). The result in the column-vector notation of (6) is

$$\tilde{\mathbf{u}} = \begin{Bmatrix} -k'R\sin k'z \\ k'R\cos k'z \\ \zeta^2 \end{Bmatrix} + \xi_0 e^{i\gamma z} \begin{Bmatrix} Rk'(k'\cos k'z + i\gamma \sin k'z) \\ Rk'(k'\sin k'z - i\gamma\cos k'z) \\ i\gamma\zeta^2 R^2 k^2 \end{Bmatrix} + \rho_0 e^{i\gamma z} \begin{Bmatrix} -k'\sin k'z + i\gamma\cos k'z \\ k'\cos k'z + i\gamma\sin k'z \\ 0 \end{Bmatrix}. \quad (7)$$

Since the unit tangent vector along the filament is

$$\mathbf{t} = \frac{d\mathbf{y}}{ds} = \frac{d\mathbf{y}}{dz}\left|\frac{dz}{ds}\right| = \mathbf{u}\frac{dz}{ds} = \frac{\mathbf{u}}{|\mathbf{u}|}$$

the relation between dz and the element of arc ds is

$$ds = |\mathbf{u}|\,dz, \quad (8a)$$

where, from (7),

$$|\mathbf{u}| = \zeta(1 + \rho_0 k'^2 R e^{i\gamma z}/\zeta^2). \quad (8b)$$

To calculate the resulting motion of a point $\mathbf{y}'$ on the vortex filament it is convenient to work in the local polar unit vectors $\mathbf{i}_r$, $\mathbf{i}_\theta$ and $\mathbf{k}$ at this point as sketched in figure 2 ($\mathbf{k}$ along y_3). The vectors $\mathbf{y}'$, $\mathbf{y}$ (the vector to any other point)

and $d\mathbf{y}$ can be expressed in components of these local unit vectors as follows:

$$\mathbf{y}' = \begin{Bmatrix} R \\ 0 \\ \zeta^2 z' \end{Bmatrix} + \xi_0 e^{i\gamma z} \begin{Bmatrix} 0 \\ -Rk' \\ R^2k^2\zeta^2 \end{Bmatrix} + \rho_0 e^{i\gamma z} \begin{Bmatrix} 1 \\ 0 \\ 0 \end{Bmatrix}, \tag{9a}$$

$$\mathbf{y} = \begin{Bmatrix} R\cos\bar{\theta} \\ R\sin\bar{\theta} \\ z\zeta^2 \end{Bmatrix} + \xi_0 e^{i\gamma z} \begin{Bmatrix} Rk'\sin\bar{\theta} \\ -Rk'\cos\bar{\theta} \\ R^2k^2\zeta^2 \end{Bmatrix} + \rho_0 e^{i\gamma z} \begin{Bmatrix} \cos\bar{\theta} \\ \sin\bar{\theta} \\ 0 \end{Bmatrix}, \tag{9b}$$

$$\mathbf{u} = \begin{Bmatrix} -k'R\sin\bar{\theta} \\ k'R\cos\bar{\theta} \\ \zeta^2 \end{Bmatrix} + \xi_0 e^{i\gamma z} \begin{Bmatrix} Rk'^2\cos\bar{\theta} + i\gamma Rk'\sin\bar{\theta} \\ Rk'^2\sin\bar{\theta} - i\gamma Rk'\cos\bar{\theta} \\ i\gamma\zeta^2k^2R^2 \end{Bmatrix} + \rho_0 e^{i\gamma z} \begin{Bmatrix} -k'\sin\bar{\theta} + i\gamma\cos\bar{\theta} \\ k'\cos\bar{\theta} + i\gamma\sin\bar{\theta} \\ 0 \end{Bmatrix}, \tag{9c}$$

where $\bar{\theta} = k'(z-z')$, the angle between $\mathbf{y}$ and $\mathbf{y}'$ (figure 2). The elements of the column vectors refer to the $\mathbf{i}_r$, $\mathbf{i}_\theta$ and $\mathbf{k}$ components respectively. The integrand of (1) is formed by vector operations on these expressions for $\mathbf{y}'$, $\mathbf{y}$ and $\mathbf{u}$. Before forming this integrand, we shall consider the kinematics of the filament motion.

2.2. *Kinematics of the filament motion*

Since the co-ordinate system rotates with angular velocity Ω_0, the total velocity of the vortex element at the point $\mathbf{y}'$ is

$$\dot{\mathbf{y}}'_{\text{tot}} = \dot{\mathbf{y}}'_{\text{rel}} + \Omega_0 \mathbf{k} \times \mathbf{y}' + V_A \mathbf{k}, \tag{10}$$

where $\dot{\mathbf{y}}'_{\text{rel}}$ is the velocity relative to the co-ordinate system in which the unperturbed helix is stationary. Taking the time derivative of $\mathbf{y}'$ from (9a), we obtain the expression for this relative velocity:

$$\dot{\mathbf{y}}'_{\text{rel}} = \dot{\xi}_0 e^{i\gamma z} \begin{Bmatrix} 0 \\ -Rk\zeta^2 \\ R^2k^2\zeta^2 \end{Bmatrix} + \dot{\rho}_0 e^{i\gamma z} \begin{Bmatrix} 1 \\ 0 \\ 0 \end{Bmatrix}. \tag{11}$$

Since the vortex element moves with the self-induced velocity, the total velocity $\dot{\mathbf{y}}'_{\text{tot}}$ of the vortex element must equal $\mathbf{q}$ (see equation (1)), the total velocity induced at the point $\mathbf{y}'$ owing to the entire perturbed vortex filament.

The differential equation for the motion of a point on the vortex filament, and thus for the growth of the perturbation amplitudes, is then

$$\dot{\mathbf{y}}'_{\text{rel}} = \mathbf{q} - \Omega_0 \mathbf{k} \times \mathbf{y}' - V_A \mathbf{k}. \tag{12}$$

Since for small ρ_0 and ξ_0 the right-hand side of (12) is homogenous and linear in ξ_0 and ρ_0, we define $\mathbf{V}_{\xi_0}$ and $\mathbf{V}_{\rho_0}$ such that

$$\xi_0 e^{i\gamma z'} \mathbf{V}_{\xi_0} + \rho_0 e^{i\gamma z'} \mathbf{V}_{\rho_0} = \mathbf{q} - \Omega_0 \mathbf{k} \times \mathbf{y}' - V_A \mathbf{k}, \tag{13}$$

where $\mathbf{V}_{\xi_0}$ and $\mathbf{V}_{\rho_0}$, the induced velocities per unit ξ_0 and ρ_0 displacement, are complex vectors which depend only on γ and kR.

The governing equations for ξ_0 and ρ_0 are then first-order linear ordinary differential equations with constant (in time) coefficients. If we assume a solution of the form $\rho_0(t) \sim e^{\alpha t}$, $\xi_0(t) \sim e^{\alpha t}$, the governing equation (12) (with (13)) becomes

$$\alpha(\mathbf{y}' - \mathbf{y}_0') = \xi_0 e^{i\gamma z'} \mathbf{V}_{\xi_0} + \rho_0 e^{i\gamma z'} \mathbf{V}_{\rho_0}, \tag{14}$$

where $\mathbf{y}_0'$ is the vector to the point on the unperturbed filament. The eigenvalue α is found by solving (14) after the coefficients $\mathbf{V}_{\xi_0}$ and $\mathbf{V}_{\rho_0}$ have been determined from (13) for a given helical filament (given k, R) and perturbation wavenumber γ. If α has a positive real part the helix is unstable; if α is purely imaginary, oscillations and waves result.

2.3. *Evaluation of the induced velocity field*

The vector operations necessary to evaluate $\mathbf{q}$ are indicated in (1). The vector $\mathbf{y} - \mathbf{y}'$, in local unit polar vectors at $\mathbf{y}'$, from (9*a*) and (9*b*) is

$$\mathbf{y} - \mathbf{y}' = \begin{Bmatrix} R(\cos\bar{\theta} - 1) \\ R\sin\bar{\theta} \\ \bar{z}\zeta^2 \end{Bmatrix} + \xi_0 e^{i\gamma z'} \begin{Bmatrix} Rk' e^{i\gamma z}\sin\bar{\theta} \\ Rk'(1 - e^{i\gamma z}\cos\bar{\theta}) \\ (e^{i\gamma\bar{z}} - 1)\,\zeta^2 k^2 R^2 \end{Bmatrix} + \rho_0 e^{i\gamma z'} \begin{Bmatrix} e^{i\gamma z}\cos\bar{\theta} - 1 \\ e^{i\gamma z}\sin\bar{\theta} \\ 0 \end{Bmatrix}, \tag{15}$$

where $\bar{z} = z - z'$ and $\bar{\theta} = k'\bar{z}$. For small ξ_0 and ρ_0, we may write the scalar in (1) as

$$\begin{aligned} \frac{1}{|\mathbf{y} - \mathbf{y}'|^3} &= \frac{1}{Y^3}\left[1 - \frac{3\xi_0 e^{i\gamma z'}}{Y^2}(1 - e^{i\gamma z})\,(k'R^2\sin\bar{\theta} - \bar{z}\zeta^4 k^2 R^2)\right. \\ &\qquad \left. - \frac{3\rho_0 e^{i\gamma z'}}{Y^2} R(e^{i\gamma\bar{z}} + 1)\,(1 - \cos\bar{\theta})\right] \\ &\equiv \frac{1}{Y^3}\left[1 - \xi_0 e^{i\gamma z'}\frac{X}{Y^2} - \rho_0 e^{i\gamma z'}\frac{Z}{Y^2}\right], \end{aligned} \tag{16}$$

where $Y = (2R^2(1 - \cos\bar{\theta}) + \zeta^4\bar{z}^2)^{\frac{1}{2}}$, the magnitude of the distance between two points on the unperturbed filament. The symbols X and Z have been introduced for the terms proportional to ξ_0 and ρ_0.

The vector cross-product $(\mathbf{y} - \mathbf{y}') \times \mathbf{u}$ is obtained directly as the cross-product of (15) and (9*c*). Retaining terms only to first order in ξ_0 and ρ_0, we have the rather lengthy expression (in components corresponding to $\mathbf{i}_r$, $\mathbf{i}_\theta$ and $\mathbf{k}$ at $\mathbf{y}'$)

$$\begin{aligned} (\mathbf{y} - \mathbf{y}') \times \mathbf{u} &= \begin{Bmatrix} R\zeta^2\sin k'\bar{z} - k'R\zeta^2 z\cos k'\bar{z} \\ R\zeta^2(1 - \cos k'\bar{z}) - k'R\zeta^2\bar{z}\sin k'\bar{z} \\ k'R^2(1 - \cos k'\bar{z}) \end{Bmatrix} \\ &\quad + \xi_0 e^{i\gamma z'} \begin{Bmatrix} \zeta^2 Rk'(1 - e^{i\gamma\bar{z}}\cos k'\bar{z}) + \zeta^2 k^2 R^3 k'\cos k'z(1 - e^{i\gamma z}) \\ \quad + (i\gamma\zeta^2 k^2 R^3\sin k'\bar{z} - Rk'^2\zeta^2\bar{z}\sin k'\bar{z} + i\gamma Rk'\zeta^2\bar{z}\cos k'\bar{z})\,e^{i\gamma} \\ - Rk'\zeta^2 e^{i\gamma\bar{z}}\sin k'\bar{z} - \zeta^2 k^2 R^3 k'\sin k'\bar{z}\,(e^{i\gamma\bar{z}} - 1) \\ e^{i\gamma\bar{z}}(-i\gamma\zeta^2 k^2 R^3(\cos k'\bar{z} - 1) + Rk'^2\zeta^2\bar{z}\cos k'\bar{z} \\ \qquad + i\gamma Rk'\zeta^2 z\sin k'\bar{z}) \\ - i\gamma R^2 k'(1 - \cos k'\bar{z})\,e^{i\gamma\bar{z}} - R^2 k'^2\sin k'\bar{z}\,e^{i\gamma\bar{z}} \end{Bmatrix} \\ &\quad + \rho_0 e^{i\gamma z'} \begin{Bmatrix} \zeta^2 e^{i\gamma\bar{z}}(\sin k'\bar{z} - k'z\cos k'\bar{z} - i\gamma\bar{z}\sin k'\bar{z}) \\ \zeta^2(1 - e^{i\gamma z}\cos k'\bar{z}) - k'\zeta^2\bar{z}\sin k\bar{z}\,e^{i\gamma\bar{z}} + i\gamma\zeta^2\bar{z}\cos k'\bar{z}\,e^{i\gamma z} \\ e^{i\gamma\bar{z}}k'R(1 - \cos k'\bar{z}) + k'R(e^{i\gamma\bar{z}} - \cos k'\bar{z}) - i\gamma R\sin k'\bar{z}\,e^{i\gamma\bar{z}} \end{Bmatrix} \\ &\equiv \boldsymbol{\chi} + \xi_0 e^{i\gamma z'}\mathbf{E} + \rho_0 e^{i\gamma z'}\mathbf{P}, \end{aligned} \tag{17}$$

where the notations $\boldsymbol{\chi}$, $\mathbf{E}$ and $\mathbf{P}$ have been introduced for the various column vectors.

The integrand of (1) (a vector) is the product of (16) (a scalar) and (17) (a vector). This product contains: (i) a zeroth-order term $\mathbf{q}_0$, the self-induced velocity of the unperturbed helix; (ii) first-order terms proportional to ξ_0 and ρ_0 which give $\mathbf{q}_1$, the induced velocity due to the perturbations and (iii) second-order terms proportional to products and squares of ξ_0 and ρ_0. These latter terms are not considered in the linear stability analysis.

The zeroth-order term in (1) becomes

$$\mathbf{q}_0 = \begin{Bmatrix} V_r \\ V_\theta \\ V_A \end{Bmatrix} = \frac{\Gamma}{4\pi}\int_{-\infty}^{\infty} \frac{1}{Y^3} \begin{Bmatrix} R\zeta^2 \sin k'\bar{z} - Rk'\bar{z}\zeta^2 \cos k'\bar{z} \\ R\zeta^2(1-\cos k'\bar{z}) - k'R\zeta^2\bar{z}\sin k'\bar{z} \\ R^2k'(1-\cos k'\bar{z}) \end{Bmatrix} d\bar{z}. \tag{18}$$

Since the $\mathbf{i}_r$ component of (18) is odd, V_r is zero. V_θ and V_A are the rotational and axial velocities of the unperturbed helix. From (18) the rotation rate Ω_0 is given by

$$\Omega_0 = \frac{V_\theta}{R} = \frac{\Gamma}{4\pi}\int_{-\infty}^{\infty} \frac{(\zeta^2(1-\cos k'\bar{z}) - k'\zeta^2\bar{z}\sin k'\bar{z})\, d\bar{z}}{Y^3}. \tag{19}$$

The first-order terms for the induced velocity due to ξ_0 and ρ_0 displacements are, apparently,

$$\mathbf{q}_1 = \frac{\Gamma}{4\pi}\xi_0 e^{i\gamma z'}\int_{-\infty}^{\infty}\left(\frac{\mathbf{E}}{Y^3} - \frac{X\boldsymbol{\chi}}{Y^5}\right)d\bar{z} + \frac{\Gamma}{4\pi}\rho_0 e^{i\gamma z'}\int_{-\infty}^{\infty}\left(\frac{\mathbf{E}}{Y^3} - \frac{Z\boldsymbol{\chi}}{Y^5}\right)d\bar{z}. \tag{20}$$

A subsequent investigation of the proper interpretation of these singular integrals will reveal that (18) contains an additional first-order contribution owing to changes in arc length along the filament due to the ρ_0 perturbation. This contribution must be added to (20) to obtain the complete induced velocity resulting from the perturbations. Before considering the evaluation of the induced velocities of (18) and (20) and the investigation of the stability of the helix to small perturbations, we shall consider an important limiting case for which the complete stability problem can be worked out analytically.

3. The stability of a helical filament from the local-induction model

In the limit of very small vortex core size, at each point the self-induced velocity due to curvature will be dominated by the nearest points on the filament. In this limit the induced velocity becomes inversely proportional to the local radius of curvature, directed along the binormal of the filament curve. The magnitude depends upon the vortex core size as $\log a$, where a is the ratio of the core radius to R, the radius of the cylinder. The limiting expression for $\mathbf{q}$, say $\mathbf{q}_l$, is then

$$\mathbf{q}_l(\mathbf{y}') \sim -\frac{\Gamma}{4\pi}\log a \frac{\mathbf{u}}{|\mathbf{u}|} \times \boldsymbol{\kappa}, \tag{21}$$

where $\boldsymbol{\kappa}$ is the curvature vector

$$\boldsymbol{\kappa} = \partial^2\mathbf{y}/\partial s^2 \tag{22}$$

and $\mathbf{u}$ and $\mathbf{y}$ are given by (9). Since $\mathbf{y}$ is a function of z, the curvature vector is obtained through the following operations:

$$\boldsymbol{\kappa} = \frac{\partial}{\partial s}\left(\frac{\partial \mathbf{y}}{\partial z}\frac{dz}{ds}\right) = \frac{\partial}{\partial s}\left(\mathbf{u}\frac{dz}{ds}\right) = \frac{\partial \mathbf{u}}{\partial z}\frac{1}{|\mathbf{u}|^2} + \frac{\mathbf{u}}{|\mathbf{u}|}\frac{\partial}{\partial z}\left(\frac{1}{|\mathbf{u}|}\right). \tag{23}$$

Straightforward calculation using (9c) results in

$$\frac{\mathbf{u}}{|\mathbf{u}|} = \begin{Bmatrix} 0 \\ kR\zeta \\ \zeta \end{Bmatrix} + \xi_0 e^{i\gamma z} \begin{Bmatrix} k^3\zeta^3 R \\ -i\gamma kR\zeta \\ i\gamma\zeta R^2 k^2 \end{Bmatrix} + \rho_0 e^{i\gamma z_2} \begin{Bmatrix} i\gamma/\zeta \\ \zeta k - \zeta^3 k^3 R^2 \\ -R\zeta^3 k^2 \end{Bmatrix} \tag{24a}$$

and

$$\boldsymbol{\kappa} = \begin{Bmatrix} -k^2 R\zeta^2 \\ 0 \\ 0 \end{Bmatrix} + \xi_0 e^{i\gamma z_2} \begin{Bmatrix} 2i\gamma Rk^2\zeta^2 \\ k^3\zeta^4 R + Rk\gamma^2 \\ -\gamma^2 k^2 R^2 \end{Bmatrix} + \rho_0 e^{i\gamma z} \begin{Bmatrix} -\gamma^2/\zeta^2 - k^2\zeta^2 + k^4\zeta^4 2R^2 \\ 2i\gamma k - i\gamma k^3\zeta^3 R^2 \\ -i\gamma\zeta^2 k^2 R^2 \end{Bmatrix}. \tag{24b}$$

The velocity $\mathbf{q}_l$ is the cross-product of (24a) and (24b):

$$\mathbf{q}_l = \frac{\mathbf{u}}{|\mathbf{u}|} \times \boldsymbol{\kappa} = \begin{Bmatrix} 0 \\ -k^2 R\zeta^3 \\ +k^3 R^2\zeta^3 \end{Bmatrix} - \xi_0 e^{i\gamma z} \begin{Bmatrix} \gamma^2 kR/\zeta + k^3\zeta^5 R \\ i\gamma\zeta^3 R^3 k^4 - 2i\gamma Rk^2\zeta^3 \\ 3i\gamma\zeta^3 k^3 R^2 \end{Bmatrix}$$

$$- \rho_0 e^{i\gamma z} \begin{Bmatrix} 2i\gamma k\zeta \\ \zeta(\gamma^2/\zeta^2 + k^2\zeta^2 - 3k^4 R^2\zeta^4) \\ -\gamma^2 \dfrac{k}{\zeta} R - 2k^3 R\zeta^3 + 3k^5 R^3\zeta^5 \end{Bmatrix}. \tag{25}$$

(For convenience, the factor $-\Gamma/4\pi \log a$ will be taken as unity in this section.) In this limiting case the angular and axial velocities of the unperturbed filament are

$$\Omega_0 = -k^2\zeta^3, \quad V_A = k^3 R^2\zeta^3. \tag{26}$$

The expression $\Omega_0 \mathbf{k} \times \mathbf{y}'$ which appears in the equation for the self-induced motion of the filament (12) is given by

$$\Omega_0 \mathbf{k} \times \mathbf{y}' = \begin{Bmatrix} 0 \\ -k^2 R\zeta^2 \\ 0 \end{Bmatrix} + \xi_0 e^{i\gamma z'} \begin{Bmatrix} -Rk^3\zeta^5 \\ 0 \\ 0 \end{Bmatrix} + \rho_0 e^{i\gamma z'} \begin{Bmatrix} 0 \\ -k^2\zeta^3 \\ 0 \end{Bmatrix}. \tag{27}$$

The equation of motion for the vortex filament is obtained from (12) using $\mathbf{y}'$ from (9), $\mathbf{q}_l$ from (25), $\Omega_0 \mathbf{k} \times \mathbf{y}'$ from (27) and V_A from (26). This results in a set of linear ordinary differential equations for the amplitudes of the perturbations, ξ_0 and ρ_0:

$$\dot{\xi}_0 \begin{Bmatrix} 0 \\ -Rk\zeta^2 \\ R^2 k^2\zeta^2 \end{Bmatrix} + \dot{\rho}_0 \begin{Bmatrix} 1 \\ 0 \\ 0 \end{Bmatrix} = -\xi_0 \begin{Bmatrix} \gamma^2 kR/\zeta \\ i\gamma\zeta^3 R^3 k^4 - 2i\gamma Rk^2\zeta^3 \\ 3i\gamma\zeta^3 k^3 R^2 \end{Bmatrix}$$

$$- \rho_0 \begin{Bmatrix} 2i\gamma k\zeta \\ \gamma^2/\zeta - 3k^4 R^2\zeta^5 \\ \gamma^2 kR/\zeta + 2k^3 R\zeta^3 - 3k^5 R^3\zeta^5 \end{Bmatrix}. \tag{28}$$

Two differential equations, each containing only $\dot{\xi}_0$ or $\dot{\rho}_0$, can be obtained from (28) by taking the scalar product of this vector equation with the orthogonal vectors $\{0, -1/Rk, 1\}$ and $\{1, 0, 0\}$. These vectors are both normal to the unperturbed filament. (The third orthogonal vector, $\{0, Rk, 1\}$, is along the unperturbed filament.) The governing equations for ξ_0 and ρ_0 then become

$$\left.\begin{aligned} \dot{\xi}_0 + 2i\gamma k\zeta\xi_0 - \{[(\gamma/\zeta)^2 - \zeta^4k^4R^2]/\zeta Rk\}\rho_0 = 0, \\ \dot{\rho}_0 + 2i\gamma k\zeta\rho_0 + (\gamma^2 kR/\zeta)\,\xi_0 = 0. \end{aligned}\right\} \tag{29}$$

The eigenvalue α, the amplification rate of the perturbations introduced in (14), is then determined by the equation

$$\begin{bmatrix} \alpha + 2i\gamma k\zeta & -[(\gamma/\zeta)^2 - \zeta^4k^2R^2]/\zeta Rk \\ \gamma^2 kR/\zeta & \alpha + 2i\gamma k\zeta \end{bmatrix} \begin{Bmatrix} \xi_0 \\ \rho_0 \end{Bmatrix} = 0. \tag{30}$$

On setting the determinant equal to zero we obtain the expression for α:

$$\alpha = (\gamma/\zeta)\,[\zeta^4k^4R^2 - (\gamma/\zeta)^2]^{\frac{1}{2}} - 2i\gamma k\zeta. \tag{31}$$

This result states that wavenumbers γ/ζ smaller than the curvature ζ^2k^2R of the unperturbed filament will be unstable; larger wavenumbers will be stable. (γ/ζ is the wavenumber based on arc length along the unperturbed filament.) The second term in (31) corresponds to waves travelling along the filament at a (non-dimensional) speed of twice the torsion of the helix. This result agrees with that obtained by Betchov (1965) using the local-induction model. For our purposes, the development in this section is a useful framework for the study of the stability problem when the influence of the entire filament is considered. The more complex expressions for the induced velocity (20) must have (25) as a limiting value for very small vortex core size. This is a very useful check in such a complex problem.

4. Evaluation and interpretation of the integrals for self-induced velocity

The integrals in the expressions for self-induced velocity of the perturbed vortex filament, (18) and (20), are singular. A proper definition and evaluation is made by considering the finite vortex core of the filament. In addition, for a general value of these integrals are not conveniently expressed in closed form and must be evaluated numerically. The most straightforward approach seems to be to separate these two difficulties, i.e. the singular behaviour and the numerical evaluation.

Each of the integrals in (18) and (20) is of the form

$$F_i(\beta) = \int_{-\infty}^{\infty} f_i(\bar{z})\, e^{i\beta\bar{z}}\, d\bar{z}. \tag{32}$$

It is convenient to identify $F_i(\beta)$ as the Fourier transform of the function $f_i(\bar{z})$ so that the numerical evaluation can be done quite efficiently using a standard fast-Fourier-transform subroutine. There are five functions that appear in the

expressions (18) and (20) for $\mathbf{q}_0$ and $\mathbf{q}_1$. These are denoted as follows:

$$\left.\begin{aligned} f_1 &= [2R^2(1-\cos k'\bar{z})+\zeta^4\bar{z}^2]^{-\frac{3}{2}}, \quad f_2 = f_1\bar{z}, \\ f_3 &= [2R^2(1-\cos k'\bar{z})+\zeta^4\bar{z}^2]^{-\frac{5}{2}}, \quad f_4 = f_1\bar{z}, \quad f_5 = f_3\bar{z}^2. \end{aligned}\right\} \tag{33}$$

The functions f_1, f_3 and f_5 are even in $\bar{z}$; f_2 and f_4 are odd.

A typical term in the velocity $\mathbf{q}$ can be represented as a sum of the transforms $F_i(\beta)$ ($i = 1$–5) with the wavenumber β taking the values $\gamma-k'$, $\gamma+k'$, $\gamma-2k'$, $\gamma+2k'$, γ, k', $2k'$ and zero. For example, the $\mathbf{i}_\theta$ component of $\mathbf{q}_0$, the tangential velocity of the unperturbed helix, becomes (from 18)

$$V_\theta = R\zeta^2[F_1(0)-F_1(k')]+ik'R\zeta^2F_2(k'). \tag{34}$$

However, the functions $f_i(\bar{z})$ are singular near $\bar{z} = 0$, so a numerical transform cannot be simply taken without a proper interpretation.

Near $\bar{z} = 0$, the functions $f_i(\bar{z})$ can be expanded as

$$f_1(\bar{z}) \sim \frac{1}{\zeta^3|\bar{z}|^3}+\frac{B}{|\bar{z}|}, \quad f_2(\bar{z}) \sim \frac{1}{\zeta^3|\bar{z}|\bar{z}}, \tag{35a}$$

where $B = R^2k'^4/8\zeta^5$, and

$$f_3(\bar{z}) \sim \frac{1}{\zeta^5|\bar{z}|^5}+\frac{C}{|\bar{z}|^3}+\frac{D}{|\bar{z}|}, \quad f_4(\bar{z}) \sim \frac{1}{\zeta^5|\bar{z}|^3\bar{z}}+\frac{C}{|\bar{z}|\bar{z}}, \quad f_5(\bar{z}) \sim \frac{1}{\zeta^5|\bar{z}|^3}+\frac{C}{|\bar{z}|}, \tag{35b}$$

where

$$C = 5R^2k'^4/(\zeta^7\times 4!) \quad \text{and} \quad D = 35(2R^2/\zeta^2)^2k'^8/[(4!)^2\,8\zeta^5]-5R^2k'^6/(\zeta^7\times 6!).$$

The evaluation and interpretation of the integrals in (32) is achieved by rewriting the integrand and adding and subtracting functions that have the same singularities as $F_i(\bar{z})$ and also can be easily treated analytically. For example, consider the function $f_1(\bar{z})$ and its transform $F_1(\beta)$. Since $f_1(\bar{z})$ is even, the right-hand side of (32) can be written as a cosine transform:

$$F_1(\beta) = 2\times\lim_{\delta\to 0}\int_\delta^\infty f_1(\bar{z})\cos\beta\bar{z}\,d\bar{z}. \tag{36a}$$

In this form we have introduced the 'cut-off' notation that will allow a proper definition of this integral in terms of the properties of the vortex core. That is, the integration is merely stopped at some small distance $\bar{z} = \delta$ from the origin $\bar{z} = 0$. The general solution (see I) for a perturbed vortex filament can be interpreted as specifying the correct choice of δ in terms of the local properties of the core.

To avoid the singularity in the numerical evaluation of $F_1(\beta)$ we rewrite (36a) as

$$\begin{aligned} F_1(\beta) = 2\times\lim_{\delta\to 0}\int_0^\infty \left(f_1(\bar{z})-\frac{1}{\zeta^3\bar{z}^3}-\frac{Be^{-\bar{z}\zeta}}{\bar{z}}\right)\cos\beta\bar{z}\,d\bar{z} \\ +2\times\lim_{\delta\to 0}\int_\delta^\infty \left(\frac{1}{\zeta^3\bar{z}^3}+\frac{Be^{-\bar{z}\zeta}}{\bar{z}}\right)\cos\beta\bar{z}\,d\bar{z}. \end{aligned} \tag{36b}$$

A comparison of (33), (35) and (36a) shows that since we have added and subtracted a function which has the same singularities as $f_1(z)$ at $\bar{z} = 0$, δ can be set to zero in the first group and the resulting non-singular integral, $G_1(\beta)$ say, evaluated numerically. (The factor $e^{-\bar{z}\zeta}$ is introduced into the $B/\bar{z}$ integral to improve convergence.)

The last integral in (36b) can be evaluated analytically in terms of the cosine integral

$$C_i(\xi) = -\int_{\xi}^{\infty} \frac{\cos x\, dx}{x}, \tag{37}$$

which for small ξ behaves like $\gamma + \log \xi$. In the limit $\delta \to 0$, $F_1(\beta)$ becomes

$$F_1(\beta) \sim G_1(\beta) + \frac{1}{\zeta^3}\left[\frac{1}{\delta^2} + \beta^2(\gamma + \log \beta\delta - \tfrac{3}{2})\right] - 2B[\gamma + \log \delta + \log (\zeta^2 + \beta^2)^{\frac{1}{2}}]. \tag{38}$$

Similar expressions can be constructed for the remaining $F_i(\beta)$'s, $i = 2$–5. This will be done shortly. However, first we shall consider both the singularities of F_1 as $\delta \to 0$ and the proper choice of δ in terms of the properties of the finite vortex core.

The induced velocity $\mathbf{q}$ is formed from various combinations of the F_i's. For a smooth vortex filament, the induced velocity is singular only as $\log \delta$, while the individual F_i's behave like $1/\delta^2$ or at most $1/\delta^4$. However, if we examine the particular combinations of F_i that appear in each term of the induced velocity we find that there is considerable cancellation. In fact, it can be shown (and must be so) that all the terms in (38) which do not contain β explicitly will cancel in forming the expression for $\mathbf{q}$ from (18) and (20). Therefore (38) can also be written as

$$F_1(\beta) = G_1(\beta) + (\beta^2/\zeta^3)(\log \beta\delta + \gamma - \tfrac{3}{2}) - B \log \zeta^2\beta^2. \tag{39}$$

Similar expressions will be derived for the remaining F_i's. All that remains to complete the evaluation of F_1 is to choose the value of δ. For this we refer to the previous results obtained in I. (See also Bliss 1970.)

In the calculation of self-induced motion of a point s on an arbitrary vortex filament, the cut-off of the Biot–Savart integral (1) a small distance l on either side of the point s will result in an expansion (in l) of the form

$$\mathbf{q}(s) \sim \frac{\Gamma}{4\pi R(s)}[-\log l\, \mathbf{n} + \mathbf{B}(s)], \tag{40}$$

where R is the local radius of curvature, $\mathbf{n}$ is the unit normal to both the local tangent and curvature vector, and $\mathbf{B}(s)$ is an $O(1)$ vector representing the effects of distant portions of the filament. In I, the solution was completed by adding a section of length $2l$ of a vortex ring of the same radius of curvature $R(s)$ at this point on the general filament to obtain an outer solution. This was then matched to a local inner solution for a curved vortex filament; the resulting self-induced motion of the vortex filament at the point s was found to be

$$\mathbf{q}(s) \sim \frac{\Gamma}{4\pi R(s)}[(-\log \tfrac{1}{2}a + A - \tfrac{1}{2})\mathbf{n} + \mathbf{B}(s)], \tag{41}$$

where A is an $O(1)$ constant. A is determined by the details of the swirl velocity v_θ; specifically,

$$A = \lim_{r/a \to \infty}\left[\int_0^{r/a} \frac{r v_\theta^2(r)\, dr}{2} - \log (r/a)\right]. \tag{42}$$

For example, if the vorticity distribution is uniform within the core and zero outside, $A = \frac{1}{4}$.

Comparison of the induced velocities from (40) and (41) shows that the correct induced velocity is obtained if the cut-off distance l is chosen such that

$$\log l = \log \tfrac{1}{2}a + \tfrac{1}{2} - A. \tag{43}$$

For the perturbed helical filament, the relation between the arc length l along the filament and the cut-off δ in the limit $\delta \to 0$ is (from (8))

$$l = \zeta(1 + \rho_0 k'^2 R\, e^{i\gamma z'}/\zeta^2)\,\delta. \tag{44}$$

From (43) and (44), the cut-off δ is chosen such that

$$\left.\begin{aligned} &\log \delta = -\log \zeta(1+\rho_0 k'^2 R\, e^{i\gamma z'}/\zeta^2) + \log a - A + \tfrac{1}{2} \\ \text{or} \quad &\log \delta \simeq \log (a/\zeta) - A + \tfrac{1}{2} - \rho_0 k'^2 R\, e^{i\gamma z'}/\zeta^2. \end{aligned}\right\} \tag{45a}$$

This result states that the proper choice of δ is affected by the perturbation ρ_0 through changes in the arc length of the perturbed filament. (This effect also occurs in the related problem of the stability of the vortex ring.) This small change in the cut-off δ need be considered only in evaluating $\mathbf{q}_0$ from (18), where it contributes a term of $O(\rho_0)$ that must be added to the first-order velocity $\mathbf{q}_1$ to obtain the complete induced velocity due to the perturbation ρ_0. Since $\mathbf{q}_1$ is already $O(\rho_0)$, δ may be chosen without taking this effect into account, i.e. with $\delta = \delta_0$, where

$$\log \delta_0 \equiv \log (a/\zeta) - A + \tfrac{1}{2}. \tag{45b}$$

We shall therefore write F_1 using $\delta = \delta_0$ and apply the necessary correction to $\mathbf{q}_0$ when it is evaluated.

F_1 is now completely defined in terms of the properties of the vortex core which enter in the combination $\log a - A$. Similar expressions for the remaining functions F_i for $i = 2$–5 follow in the same manner. Again, in the limit $\delta \to 0$, all terms more singular than $\log \delta$ must cancel when $\mathbf{q}$ is formed, so these terms and all terms which do not contain β may be eliminated from the F_i's at the outset. Hence

$$\left.\begin{aligned} F_2(\beta) &= G_2(\beta) - (2\beta i/\zeta^3)\{\log(\beta\tilde{a}/\zeta) - 1\}, \\ F_3(\beta) &= G_3(\beta) - (\beta^4/12\zeta^5)\{\log(\beta\tilde{a}/\zeta) - \tfrac{3}{2} - \tfrac{1}{3} - \tfrac{1}{4}\} \\ &\qquad + C\beta^2\{\log(\beta\tilde{a}/\zeta) - \tfrac{3}{2}\} - D\log(\zeta^2+\beta^2), \\ F_4(\beta) &= G_4(\beta) + (i\beta^3/3\zeta^5)\{\log(\beta\tilde{a}/\zeta) - \tfrac{3}{2} - \tfrac{1}{3}\} - 2i\beta C\{\log(\beta\tilde{a}/\zeta) - 1\}, \\ F_5(\beta) &= G_5(\beta) + (\beta^2/\zeta^5)\{\log(\beta\tilde{a}/\zeta) - 1\} + C\log(\zeta^2+\beta^2), \end{aligned}\right\} \tag{46}$$

where $\log \tilde{a} = \log a - A + \tfrac{1}{2}$ and C and D are defined by (35b). The functions G_i are given by the expressions

$$\left.\begin{aligned} G_2(\beta) &= \int_{-\infty}^{\infty} \left(f_2(\bar{z}) - \frac{1}{\zeta^3|\bar{z}|\bar{z}}\right) e^{i\beta\bar{z}}\, d\bar{z}, \\ G_3(\beta) &= \int_{-\infty}^{\infty} \left(f_3(\bar{z}) - \frac{1}{\zeta^5|\bar{z}|^5} - \frac{C}{|\bar{z}|^3} - \frac{D\, e^{-|\zeta\bar{z}|}}{|\bar{z}|}\right) e^{i\beta\bar{z}}\, d\bar{z}, \\ G_4(\beta) &= \int_{-\infty}^{\infty} \left(f_4(\bar{z}) - \frac{1}{\zeta^5|\bar{z}|^3\bar{z}} - \frac{C}{|\bar{z}|\bar{z}}\right) e^{i\beta\bar{z}}\, d\bar{z}, \\ G_5(\beta) &= \int_{-\infty}^{\infty} \left(f_5(\bar{z}) - \frac{1}{\zeta^5|\bar{z}|^3} - \frac{C}{|\bar{z}|} e^{-|\zeta\bar{z}|}\right) e^{i\beta\bar{z}}\, d\bar{z}. \end{aligned}\right\} \tag{47}$$

As can be seen by comparing (33), (35) and (47), the integrands of the G_i's are formed by subtracting from the f_i's simple functions that have the same singularities. The resulting non-singular integrals can easily be evaluated numerically to give the G_i's. The remaining singular integrals in F_i are then treated analytically as cut-off integrals and evaluated with δ chosen according to (45*b*) to give the complete expression (46).

5. Calculation of induced velocities and evaluation of stability characteristics

Now that the singular integrals (32) have been defined in terms of the properties of the finite vortex core, the induced velocities due to the perturbations can be calculated. The zeroth-order integral for $\mathbf{q}_0$, equation (18), is considered first. Because the choice of the cut-off δ is affected by the perturbation ρ_0, $\mathbf{q}_0$ contains both the self-induced motion of the unperturbed helical filament and a first-order term proportional to ρ_0. The expression for $\mathbf{q}_0$ in terms of the F_i's, from (18), is

$$\mathbf{q}_0 = [R\zeta^2(F_1(0)-F_1(k'))+ik'R\zeta^2F_2(k')]\,\mathbf{i}_\theta+k'R^2(F_1(0)-F_1(k'))\mathbf{k} \\ -\rho_0\frac{k'^4R^2e^{i\gamma z'}}{\zeta^3}\mathbf{i}_{\theta'}+\rho_0\frac{k'^5R^3}{\zeta^5}e^{i\gamma z'}\mathbf{k}. \quad (48)$$

The small correction terms must be added to $\mathbf{q}_0$ since the definition of F_i contains only the lowest order expression for δ, equation (45*b*), whereas in evaluating (18) the full expression (45*a*) must be used. The first-order correction is

$$\mathbf{q}_0' = -\rho_0\frac{k'^4R^2}{\zeta^3}e^{i\gamma z'}\mathbf{i}_\theta+\rho_0\frac{k'^5R^3}{\zeta^5}e^{i\gamma z'}\mathbf{k}. \quad (49)$$

This term is added to $\mathbf{q}_1$ as given by (20) to obtain the complete induced velocity at a point on the filament resulting from the perturbation ρ_0.

Owing to the complexity of the expression (20) for $\mathbf{q}_1$, it does not seem worthwhile to rewrite $\mathbf{q}_1$ as a function of the F_i's. Although the resulting expression is very long, the various terms can be obtained by inspection using the definitions of F_i from (32). For example, a typical term in $\mathbf{q}_1$ can be written as

$$\int_{-\infty}^{\infty}\frac{e^{i\gamma\bar{z}}\cos k'\bar{z}}{Y^3} = \tfrac{1}{2}[F_1(\gamma+k')+F_1(\gamma-k')].$$

In the stability calculations the induced velocities were directly programmed using the expression (46) for the F_i's and numerical values for the G_i's as calculated from (47) by means of a standard fast-Fourier-transform subroutine. The wavenumber β takes the values $\gamma+k'$, $\gamma+2k'$, γ, k', $2k'$ and zero in the expression for the induced velocity. One useful check on the numerical calculation of the induced velocity is that those terms proportional to $-\log a$ (each F_i contains $\log a$) must be equal to the induced velocity given by the local-induction model (25). That these terms formed from the F_i's did agree numerically with the limiting values gives some confidence in the details of the computation.

The total induced velocity due to the perturbations may then be written as

$$\mathbf{q}_T = (\Gamma/4\pi)\,[\mathbf{q}_l(-\log a + A) + \mathbf{q}_g + \mathbf{q}_0'], \tag{50}$$

where $\mathbf{q}_l$ is the limiting self-induced velocity from the local induction model (25), $\mathbf{q}_g$ is due to distant portions of the filament (obtained numerically) and $\mathbf{q}_0'$, from (49), is the correction due to the perturbation of the cut-off δ.

There are two possible models for the behaviour of the core during the perturbation. For one it is assumed that variations in the core size along the filament will be resisted by very small-scale processes within the core,† i.e. flow along the filament due to changes in the interior pressure produced by changes in core size, so that, for $\gamma \neq 0$, a is taken as a_0. (The $\gamma = 0$ mode is a special case. This mode is neutrally stable and just represents the response of a helix to a change in radius; it translates at a new velocity.) In the other model it is assumed that each element of the vortex filament will conserve volume so that $a^2(s)\,l(s)$ remains constant during the perturbation.

In the related study of the stability of the vortex ring (II) both of these models for vortex core behaviour were considered. The results showed that amplication rates obtained by assuming that the core radius was constant were only about 8 % higher than those obtained assuming that the local volume was constant. In this study we shall assume that a remains constant along the filament during the perturbation.

We have completed our description of the evaluation of the total self-induced velocity at a point on the perturbed helical vortex filament as given by (1); the expression for $\mathbf{q}$ is

$$\mathbf{q} = V_A\mathbf{k} + R\Omega_0\mathbf{i}_\theta + \mathbf{q}_T, \tag{51}$$

with $\mathbf{q}_T$ taken from (50), Ω_0 from (19) and V_A from (18). This expression contains not only the effect of the local radius of curvature but also the effects of the entire (perturbed) filament as well as the effects of vortex core size and vorticity distribution within the core. As to its limits of applicability, the core size a should be small in comparison with both the local radius of curvature of the unperturbed filament $\mathscr{R}$ ($\mathscr{R} = (Rk^2\zeta^2)^{-1}$ from (24)) and the wavelength of the perturbation.

The stability analysis proceeds as did the analysis of § 2, equations (27)–(31), which used the local induction model to evaluate $\mathbf{q}$ rather than the full expression (51). The governing equation for the perturbation amplitudes ξ_0 and ρ_0 is again given by (12). The expression $\Omega_0\mathbf{k}\times\mathbf{y}$, which appears in (12), is again given by (27) but now Ω_0 is determined by (19) rather than by (26). The scalar products of the resulting kinematic equations, analogous to (28), with orthogonal vectors (see § 2) are then taken to produce a set of linear ordinary differential equations for ξ_0 and ρ_0.

We define a non-dimensional amplification rate $\bar{\alpha}$ as

$$\bar{\alpha} = \alpha/(\Gamma/4\pi R^2),$$

where α is as in (14). The resulting eigenvalue problem for $\bar{\alpha}$ (corresponding to (30)) is of the form

$$\begin{bmatrix} \bar{\alpha} + iQ_{\xi\xi} & Q_{\xi\rho} \\ Q_{\rho\xi} & \bar{\alpha} + iQ_{\rho\rho} \end{bmatrix} \begin{Bmatrix} \xi_0 \\ \rho_0 \end{Bmatrix} = 0. \tag{52}$$

† This model was suggested to the author by Dr Phillip Saffman.

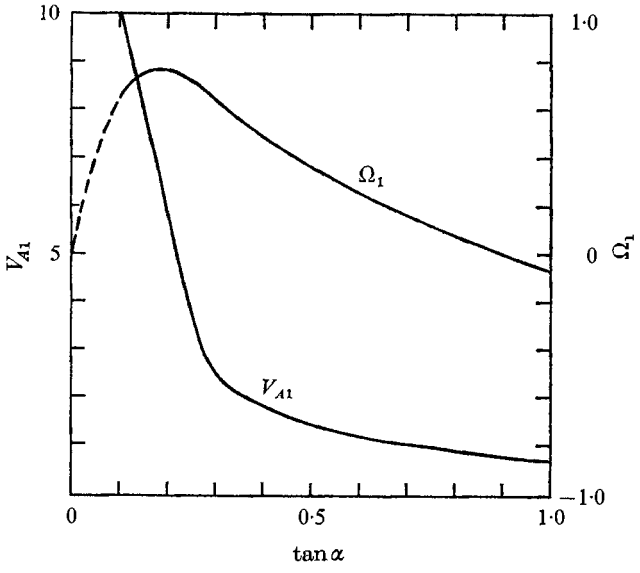

FIGURE 3. The $O(1)$ contributions V_{A1} and Ω_1 to the axial and rotational velocities of the helix as defined by (53) and (54).

All the Q's turn out to be real. Since the induced velocity $\mathbf{q}_T$ and the velocity $\mathbf{q}_l$ from the local-induction model (25) are related through (50), each element Q of the matrix in (52) is the sum of the corresponding element from (30) multiplied by $-\log a + A$ plus an $O(1)$ term due to the more distant portions of the filament, e.g. a typical term $Q_{\rho\xi}$, is

$$Q_{\rho\xi} = (-\log a + A)\gamma^2 kR/\zeta + \bar{Q}_{\rho\xi}.$$

From (52),

$$\bar{\alpha} = -i(Q_{\rho\rho} + Q_{\xi\xi}) \pm \tfrac{1}{2}(4Q_{\rho\xi}Q_{\xi\rho} - (Q_{\xi\xi} - Q_{\rho\rho})^2). \tag{53}$$

Although it is not obvious from the full expressions for $Q_{\rho\rho}$ and $Q_{\xi\xi}$, these turn out to be numerically equal. Before discussing the numerical results for $\bar{\alpha}$, we shall consider another useful limiting case provided by $\gamma = k'$.

The displacement $\rho_0 e^{ik'z}$ corresponds to a sideways displacement of the helix without distortion. Since the undeformed helix rotates with an angular velocity Ω_0, to an observer fixed at a point on the filament this perturbation will appear to rotate at $-\Omega_0$. Therefore for $\gamma = k'$, $\bar{\alpha}$ should equal $i\Omega_0$. The fact that the numerical calculations did indeed give this result for all values of kR and the vortex core radius a served as a rather thorough and final numerical check. It is interesting that this case, $\gamma = k'$ (or the $n = 1$ mode), was the only case considered by Levy & Forsdyke (1928) in their early treatment of the stability of the helical filament. They obtained results which showed that the perturbation mode $\gamma = k'$ is stable for a pitch ($\tan\alpha$) greater than 0·3 and unstable for a pitch below 0·3. In fact, this mode must always be stable since the ρ_0 perturbation represents no deformation. However, owing to the difficulty associated with the proper treatment of the finite vortex core and the requirement for extensive numerical computation, it is not too surprising that these results were inaccurate.

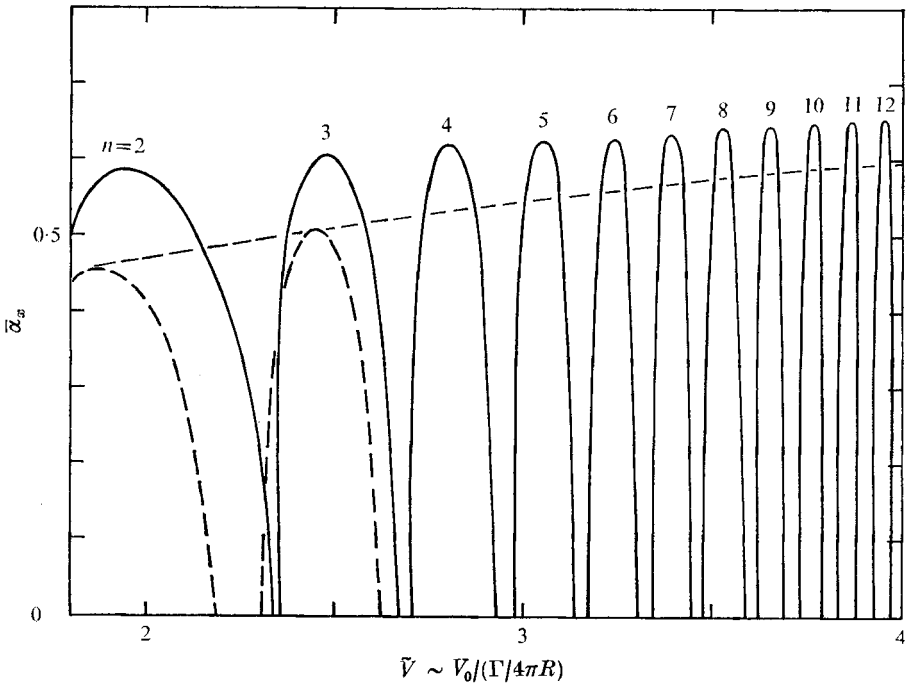

FIGURE 4. Spatial amplification rate *vs.* vortex core parameter $\tilde{V}$ for a vortex ring with an instability mode of n waves around the perimeter ——, results assuming the core size a remains constant during the perturbation; – – – –, the results and the envelope of the results assuming constant local volume for the vortex filament.

The axial and rotational velocities of the unperturbed helix are of the form

$$V_A = (\Gamma/4\pi R)\,[-V_{Al}(\log a/R - A) + V_{A1}] \tag{54}$$

and

$$\Omega_0 = (\Gamma/4\pi R^2)\,[-\Omega_l(\log a/R - A) + \Omega_1], \tag{55}$$

where $V_{Al} = k^3R^3\zeta^3$ and $\Omega_l = -k^2R^2\zeta^3$ from (25), and V_{A1} and Ω_1 (obtained numerically) are $O(1)$ functions which depend only upon kR. V_{A1} and Ω_1 are shown in figure 3 as a function of the pitch of the underformed helix ($\tan\alpha = 1/kR$). These results agree with previous work on the motion of helical vortex filaments reported by Loukakis (1971) in a study of marine propeller wakes.

Before presenting the stability results for the helical filament we present the related results for the vortex ring, taken from II. For a vortex ring, the induced velocity V_0 divided by $\Gamma/4\pi R$ is a very useful parameter for characterizing the properties of the finite core because it contains only the effects of core size and vorticity distribution. From the formula for the self-induced velocity V_0 of a vortex ring (e.g. from I) we find this parameter $\tilde{V}$ to be

$$\tilde{V} = V_0/(\Gamma/4\pi R) = \log(8R/a) + A - \tfrac{1}{2}.$$

Since γ must be an integer for the vortex ring, the amplification rate $\bar{\alpha}$ is expressed as a function of $\tilde{V}$ for the various modes, corresponding to $\gamma = n$. In II, results are presented for the spatial amplification rate, the growth rate $\bar{\alpha}_x$ of the

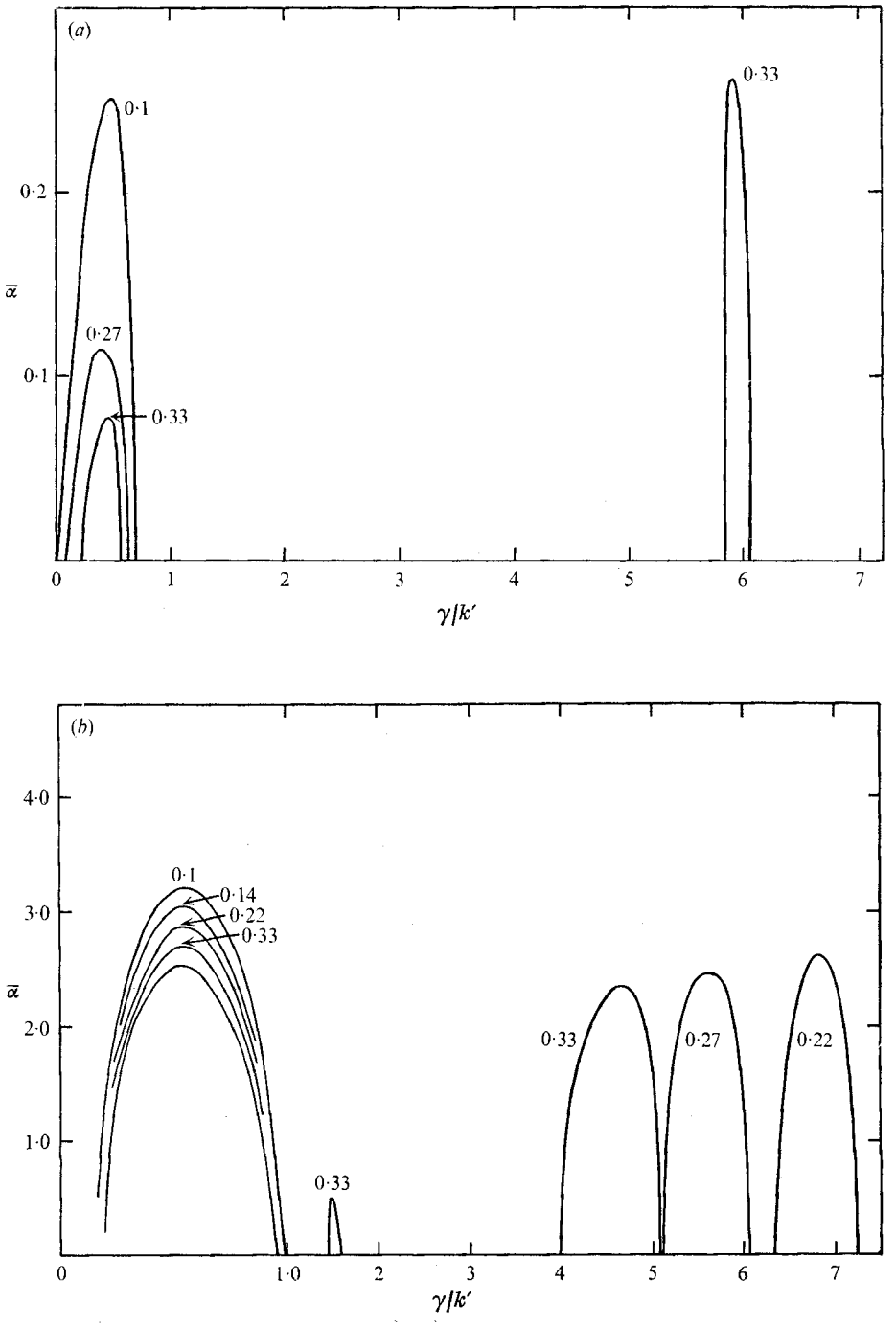

FIGURE 5*a* and 5*b*. For legend see opposite page.

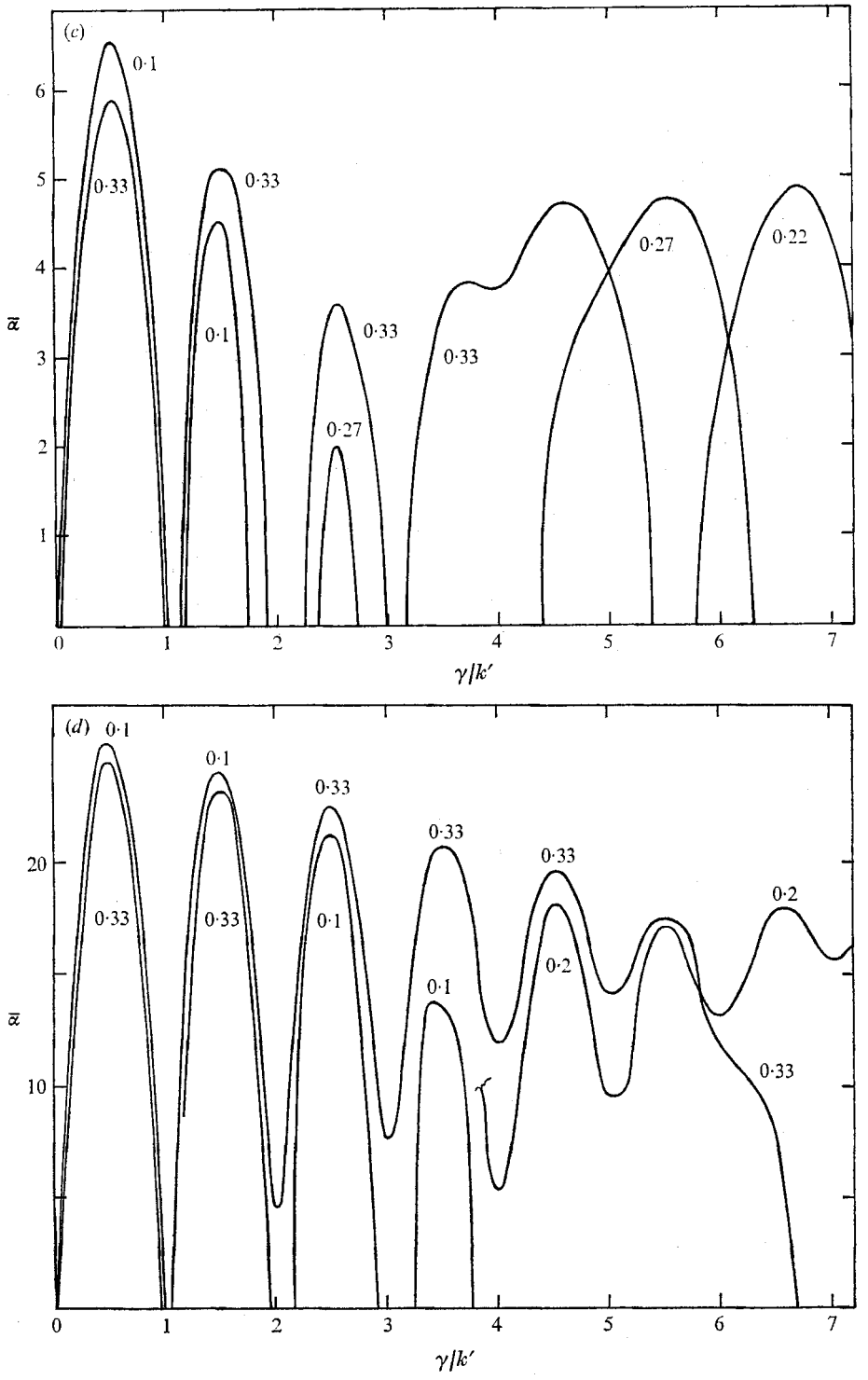

FIGURE 5. Non-dimensional amplification rate for helices with various values of $\tan\alpha$ (the pitch) with an instability mode of γ/k' waves per cycle. The values of the ratio of vortex core radius to cylinder radius are shown on each curve. (*a*) $\tan\alpha = 1$; (*b*) $\tan\alpha = 0{\cdot}3$; (*c*) $\tan\alpha = 0{\cdot}2$; (*d*) $\tan\alpha = 0{\cdot}1$.

instability with distance (in radii) travelled by the ring, obtained by multiplying α with R/V_0.

$$\bar{\alpha}_x = \alpha R/V_0. \tag{56}$$

Figure 4 shows $\bar{\alpha}_x$ as a function of $\tilde{V}$.

For each mode of deformation, with n waves around the perimeter, there is a range of $\tilde{V}$ for which $\bar{\alpha}_x$ is real and positive (instability). For large $\tilde{V}$ (small core size), the unstable mode contains many wavelengths. This makes it more difficult to justify our application of perturbation techniques, since the core size should be small in comparison with both the radius and the wavelength of the instability. However, there is experimental evidence (Krutzsch 1939) that the vortex ring of small core size does exhibit an instability with many waves around the perimeter, so that this result is at least qualitatively correct.

One suspects that the short-wave instability is a local property of a curved vortex filament and is not restricted to the ring since for very short waves only the influence of neighbouring portions of the filament would be important. (It is, however, necessary to go to $O(1)$ in calculating the induced velocities since the $O(-\log a)$ terms do not indicate instability.) Since γ may take any value on the helical filament, we would expect for a given core size to find a range of γ for which a short-wave instability exists. Of course, since the helix is more complex and neighbouring filaments interact, other longer wave instabilities are also possible. In the limit of very small core size, (31) shows that wavenumbers smaller than the local curvature are unstable. These waves cannot exist on the ring but are allowed on the helix.

Numerical calculations were performed for helix pitches, $\tan\alpha$, of 1·0, 0·4, 0·3, 0·2, 0·13 and 0·1. The results of the stability calculations, the non-dimensional amplification rates as a function of wavenumber, are shown in figure 5 for helices of various pitch and various vortex core radii. The vorticity in the core has been taken as uniform, so that $A = \frac{1}{4}$. The parameter γ/k', the number of waves per cycle of the helix, is used to characterize the perturbation mode. Although the core size is assumed to be small, here we have presented results for a ranging from 0·01 to 0·33 to indicate the general trends.

The most interesting result of the stability calculations is that there are three distinct types of instability of the helical vortex filament. On considering the general features of figures 5 (*a*)–(*d*) we see the following:

(i) There exists a very short-wave instability mode, analogous to the short-wave instability of the vortex ring. For this mode the local radius of curvature of the helix R is the characteristic length, so that in comparing the details to the ring solution one should use aR/R as a measure of vortex core size, $(\gamma/k')(\mathscr{R}/R)$ as a measure of effective 'n', and $\bar{\alpha}(\mathscr{R}/R)^2$ as a measure of the amplification rate.

(ii) For $\gamma/k' < kR$, a low wavenumber instability exists. This is also the neutral stability boundary (from (31)) obtained if the local-induction model is used to calculate the induced velocities. Although the general characteristics of the instability are as predicted by (31), namely increasing amplification rate with decreasing core size with the most unstable wave occurring at about

$$\gamma/k' = kR\zeta/\sqrt{2},$$

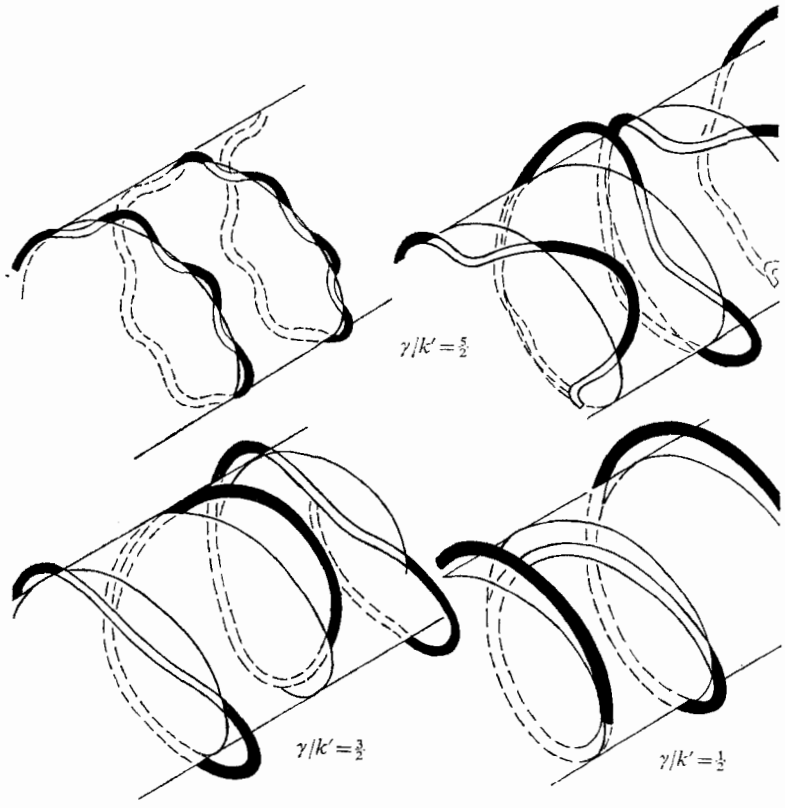

FIGURE 6. Instability mode shapes; the short-wave instability, the mutual-inductance modes with $\gamma/k' = \frac{5}{2}$ and $\frac{3}{2}$ and the long-wave instability with $\gamma/k' = \frac{1}{2}$. The last three curves were plotted from numerical computations. The dark portions are outside the cylinder on the near side; the light portions are inside.

the $O(1)$ terms are very important in determining the magnitude of $\bar{\alpha}$, typically yielding values greater by factors of 3 or 4 than those given by (31).

(iii) For values of helical pitch such that successive turns pass within a distance of one radius (say $\tan\alpha \leqslant 0{\cdot}3$), a third instability appears owing to mutual inductance between the turns. This is analogous to the vortex pair instability but differs in that the circulation of 'each filament' is the same. Referring to figure 5(*b*), for which $\tan\alpha = 0{\cdot}3$, we see a weak instability at $\gamma/k' = \frac{3}{2}$ for $a/R = 0.33$. In figure 5(*c*), for which $\tan\alpha = 0{\cdot}2$, this instability is much more prominent and occurs at both $\gamma/k' = \frac{3}{2}$ and $\frac{5}{2}$. The significance of these wave-numbers is that the perturbation is 180° out of phase on successive turns and the mode shape is similar to the vortex-pair instability. In this mutual-induction instability mode, decreasing vortex core size leads to decreasing amplification rate.

The mode shape can be obtained from (51). Since $Q_{\xi\xi}$ is equal to $Q_{\rho\rho}$,

$$\bar{\alpha} = -iQ_{\xi\xi} + \bar{\alpha}_R$$

and therefore

$$\xi_0 = -(Q_{\xi\rho}/\bar{\alpha}_R)\rho_0,$$

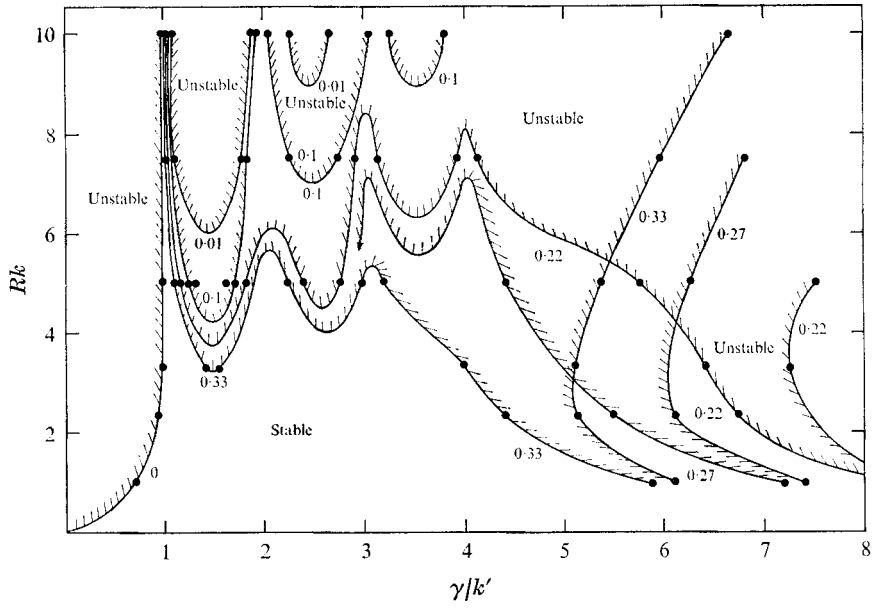

FIGURE 7. Stability boundaries for helical vortex filaments of finite core. The value of the ratio of core-to-cylinder radius are shown on each curve. Above the boundary, the helical filament of that core size is unstable.

where $\bar{\alpha}_R$ is the real part of $\bar{\alpha}$. A sketch of typical mode shapes for the various instabilities, given in figure 6, shows the short-wave instability, the mutual-inductance modes, with $\gamma/k' = \frac{5}{2}$ and $\frac{3}{2}$ and the long-wave instability, with $\gamma/k' = \frac{1}{2}$. With the mutual-inductance instability the neighbouring filaments attempt to roll up around one another as do the vortices in a pair of the same sign or in the vortex sheet from a wing.

The stability boundaries for several vortex core radii appear in figure 7. For each value of the vortex core radius, the neutral stability curve is shown, i.e. γ/k' as a function of kR for which the amplification rate $\bar{\alpha}$ is zero. To the right of this curve $\bar{\alpha}$ is real and positive; the filament is unstable. For $\gamma/k' < 1$, the local-induction model gives the neutral curve for a vortex core radius a of zero; $\gamma/k' = kR/(1+k^2R^2)^{\frac{1}{2}}$. For all practical purposes, this is also the neutral curve for $a > 0$.

The general trends of the stability boundary for a given core size are as follows: for kR below some critical value two instability modes are present, the short-wave mode and the local-induction instability; with increasing kR (decreasing pitch), the mutual-inductance modes become unstable; with further increases in kR the mutual-inductance modes merge and the helix is unstable for almost all wavelengths. It is always stable for $\gamma/k' \equiv 1$ and there is an upper boundary for the short-wave instability for any given vortex core size.

In the limit $kR \to \infty$ the helix becomes a jet, which is unstable for all wavenumbers, but this limit must be carefully taken so that Γ becomes a differential quantity as $kR \to \infty$. Also, the interpretation of the single filament and finite core would have to be carefully considered. This will not be done.

6. Conclusions

We have demonstrated that the helical vortex filament of finite core size is unstable to small sinusoidal displacements of the filament, especially as the pitch becomes small and neighbouring filaments can strongly interact. The analysis considers the effect of the entire perturbed vortex filament on the self-induced motion of each element. The formulation is general and can be used for any distribution of vorticity within the core. Since the solution for self-induced motion of the vortex filament from I includes the effects of axial velocity within the core, this could also be considered in the analysis.

However, to test these results experimentally requires some additional considerations. A single helical filament is a difficult flow to create. A propeller or helicopter wake has one helical filament trailing from each blade. In addition, since the lift drops to zero at the hub, there is probably vorticity of opposite sign shed along the blade, inboard from the tip. Also, since a propeller can create no net circulation downstream there must at least be a hub vortex equal in strength to all of the filaments. The effect of these vortex filaments on the stability of the total configuration would have to be examined in each case. It is likely, though, that in spite of these complications instabilities will be observed in these situations.

If desired, a single helical filament could be created, for example, by rotating a long cylindrical tube containing a mean flow with a wing section mounted on one wall extending along a radius but ending before the centre-line.

This work was supported by Air Force Office of Scientific Research (OSR) under contract F44620-69-C-0090.

REFERENCES

BETCHOV, R. 1965 On the curvature and torsion of a vortex filament. *J. Fluid Mech.* **22**, 471–479.

BLISS, D. B. 1970 The dynamics of curved rotational vortex lines. M.S. Thesis, Massachusetts Institute of Technology.

KRUTZSCH, C. H. 1939 Über eine experimentell beobachtete Erscheining an Werbelringen bei ehrer translatorischen Beivegung in Werklechin. *Flussigheiter Ann. Phys.* 5. Folge Band 35, 497–523.

LEVY, H. & FORSDYKE, A. G. 1928 The steady motion and stability of a helical vortex. *Proc. Roy. Soc.* A **120**, 670–690.

LOUKAKIS, T. A. 1971 A theory for the wake of Marine propellors. ScD. Thesis, Department of Naval Architecture and Marine Engineering, Massachusetts Institute of Technology.

SAFFMAN, P. G. 1970 The velocity of viscous vortex rings. *Studies in Appl. Math.* **49**, 370–380.

WIDNALL, S. E., BLISS, D. B. & ZALAY, A. 1970 Theoretical and experimental study of the stability of a vortex pair. *Proceedings of the Symposium on Aircraft Wake Turbulence, Seattle.* Plenum Press.